Evaluation of wind loads on solar panel modules using CFD

3 authors, including:

G. T. Bitsuamlak
The University of Western Ontario
137 PUBLICATIONS **1,014** CITATIONS

SEE PROFILE

Evaluation of wind loads on solar panel modules using CFD

Girma T. Bitsuamlak[a], Agerneh K. Dagnew[b], James Erwin[c]
[a,b,c]*Laboratory for Wind Engineering Research, International Hurricane Research Center/ Civil and Environmental Engineering Department, FIU, Miami, Florida, bitsuamg@fiu.edu*

ABSTRACT: Due to the growing interest in alternative energy sources, the demand for solar energy technologies in Florida, "the Sunshine State," and around the United States is on the rise. The existing types of technology, methods of installation, and mounting locations (ground, roof, or integrated with the building envelope) vary significantly, and are consequently affected by wind loads differently. The present study attempted to investigate the aerodynamic features of ground-mounted solar panels under atmospheric boundary layer flows using two techniques of computational fluid dynamics (CFD): the Reynolds Averaged Navier Stokes (RANS) equations turbulence modeling approach adapted to obtain initial conditions for use by the more reliable Large Eddy Simulation (LES) technique. The CFD results have been compared and validated with a full-scale experimental measurement performed at the Wall of Wind (WoW) testing facility at Florida International University (FIU). In addition to depicting detail aerodynamic flow characteristics such as flow separation and sheltering effects etc that can provide a better insight to designers, the LES results showed good agreement on the pressure distribution patterns and in some cases on the magnitude as well when compared with the full-scale measurements. Overall the LES underestimated the mean pressures compared to the full-scale measurements.

KEY WORDS: Wind load, computational fluid dynamics, Full-scale, sheltering effect, LES, turbulence, solar panel.

1 INTRODUCTION

The current impetus for alternative energy sources is increasing the demand for solar energy technologies in Florida, "the Sunshine State," and around the United States. The existing types of technology, methods of installation, and mounting locations (ground, roof, or integrated with the building envelope) vary significantly, and are consequently affected by wind loads differently. Considering the high demand for solar power and the variations among the solar technologies available on the market, only a limited number of wind tunnel and numerical studies exist on the subject of solar panel aerodynamics. Chevalien and Norton (1979) performed a wind tunnel study investigating the sheltering effect on a row of solar panels mounted on a model building. Kopp et al. (2002) conducted experimental studies on the evaluation of wind-induced torque on solar arrays arranged in parallel, and showed that, for a separation close to the critical value where the onset of wake buffeting was anticipated, the peak aerodynamically-induced system torque was observed at a 270^0 wind angle of attack due to the formation of vortex shedding from the upstream modules. Chung et al (2008) carried out an experimental study to investigate the wind uplift and mean pressure coefficient on a solar collector model installed on the roof of buildings under typhoon-type winds. The study found that the uplift force could be effectively reduced by using a guide plate normal to the incident wind direction, and by adopting a lifted model. It also demonstrated that pronounced local effects started around the front edge and decrease near a distance of one-third from the leading edge. Recent advances in hardware and

software technology and numerical modeling are encouraging widespread applications of computational fluid dynamics (CFD) in wind engineering. Significant progress has been made in the application of computational wind engineering (CWE) to evaluate wind loads on short and tall buildings (to name some, Murakami and Mochida, 1988; Stathopoulos, 1997; Camarri et al., 2006; Tamura et al., 2008; Tutar and Celik, 2007; El-Okda et al., 2008; Tominaga et al., 2008; Dagnew et al., 2009 and others). Following similar principle, Shademan and Hangan (2009) employed a CFD simulation to estimate wind loads on stand-alone and arrayed solar panels engulfed in a turbulent wind field. The study identified locations experiencing maximum wind-induced effects and also indicated that a critical spacing, S, of X/D=1 between panels in a tandem arrangement, created a sheltering phenomenon yielding the minimum drag force on the downstream panels. Extreme wind events such as hurricanes present additional challenges in the design of solar panels. Aerodynamic forces resulting from the drag and uplift effects caused by extreme winds acting on stand-alone solar panels and arrays can cause considerable damage, thereby reducing their efficiency and possibly creating the need for costly maintenance or replacement unless properly accounted for during the design process. Detached solar panels may also become a source of wind-borne debris if they are not properly installed. Additionally, wind performance considerations will have a significant impact when determining the optimal geometrical configuration of solar panels. These challenges, coupled with a lack of clear guidelines on wind loading criteria for solar panels, is hindering their use in the coastal, hurricane-prone regions of the US.

2 CFD SIMULATION CASES

For this study, CFD techniques were used to investigate the aerodynamic features of stand-alone ground mounted solar panels modules (maximum PV panel height H = 1.3m)under an atmospheric boundary layer flow. A typical 40˚ panel inclination angle was considered in the present work. The wind loads for an individual solar panel module were evaluated under three different incident angles of attack, followed by interference analysis by considering three modules arranged in a 3x1 array. The CFD simulation cases are listed in Table 1. As a preliminary study, the CFD simulation employed Reynolds Averaged Navier Stokes (RANS) equations with the objective of producing initial conditions for the computationally intensive but more reliable Large Eddy Simulation (LES) technique.

Table 1 CFD simulation cases

Cases	Panel type	Panel inclination	Angle of attack	No. of grid cells
Case A	Stand-alone	40˚	180˚	2.60×10^6
Case B	Stand-alone	40˚	0˚	2.95×10^6
Case C	Stand-alone	40˚	30˚	1.02×10^6
Case D	Arrayed	40˚	0˚	1.68×10^6

3 EXPERIMENTAL MEASURMENTS

To validate the CFD simulations, an experiment was conducted at Florida International University's (FIU) Wall of Wind (WoW) facility to measure the wind-induced pressures along a vertical line of pressure taps located on a ground-mounted solar panel unit (Figs 1a, b and c). The test se-

tup consisted of an aluminum solar panel frame, inclined at approximately 40˚ with respect to the longitudinal direction of mean wind flow. Two 1300 mm x 1100 mm x 19 mm (l x w x d) pieces of plywood were attached to the aluminum frame, simulating the photovoltaic panels (Fig. 1b). The thickness of the plywood provided a sufficient platform to install pressure tubes, made of 9.525 mm inner diameter (ID) flexible tubing, and mounted flush with the surface of the wood (Fig. 1c) without changing the aerodynamic (shape) characteristics of the panel. A total of 11 pressure taps were placed on the solar panel model, along the line indicated in Fig. 1b, which measured 775 mm from the outer edge of the panel. The 3-min WoW quasiperiodic waveform developed by (Huang et al. 2009) generated the ABL-like velocity profile and turbulence conditions during the full-scale experiments. Tests were conducted with two wind angles of incidence: 180˚ (similar to CFD's Case A) and 0˚ (similar to CFD's Case B). Two Turbulent Flow Instrumentation (TFI) cobra probes were placed on each side of the solar panel test setup, at heights of 510 mm and 1220 mm, to record the u, v, and w components of the oncoming wind during the full-scale experiments. WoW mean pressure coefficients, C_p, are shown in Figs 2a and b. The mean wind speeds measured during the experiments are also shown in Fig. 3a.

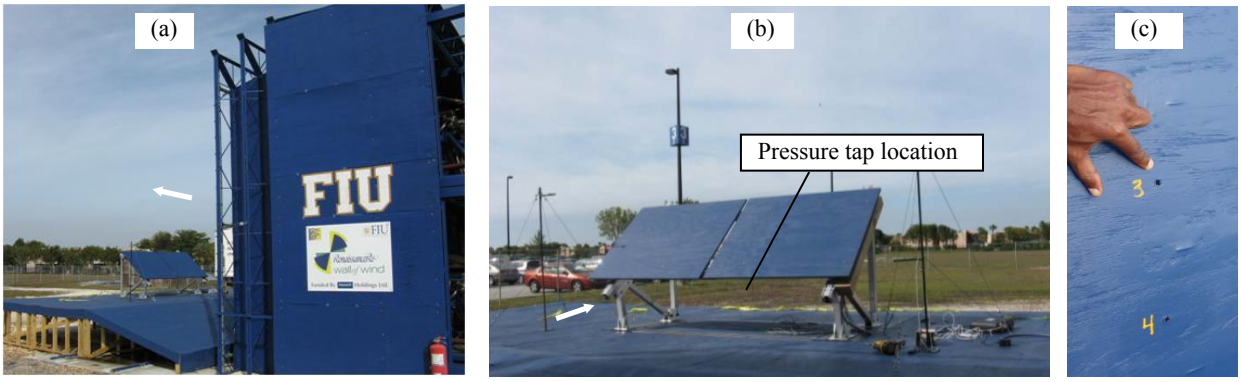

Fig 1 (a) Full-scale ground mounted solar panel setup, (b) close-up view of the solar panel and location of the pressure tap line on the solar panel, and (c) close-up view of pressure tap installed on plywood sheet.

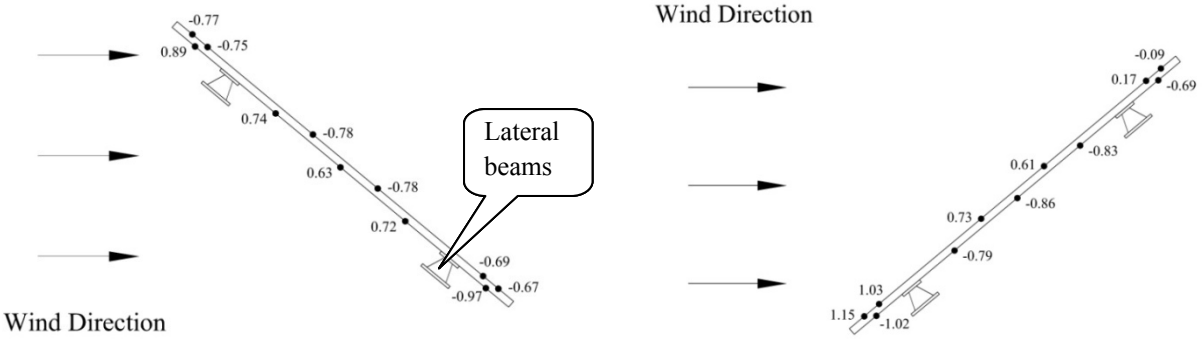

Fig 2 Mean pressure coefficient (Cp) results from WoW full-scale experiments: (a) 180^0 and (b) 0^0 angle of attack

4 NUMERICAL MODELING

The computational domain (CD) for both the stand-alone and arrayed solar panel simulation cases considered a large enough domain to minimize effects due to blockage in the numerical results and use consistent boundary conditions. An open terrain power law (α=0.15) wind speed profile with mean wind speed 50 m/sec measured at 10 m from the ground and a turbulence intensity (TI) of 16% were applied at the inlet plane of the flow domain (Fig. 3a). No-slip wall functions were used at the ground and solar panel surfaces of the computational domain. Symmetry boundary was applied to the lateral and top surfaces of the CD, since the flow is parallel to these surfaces. At the outlet plane located downstream from the solar panel, an outflow boundary condition was imposed, which assumes zero gradients for all flow variables. The main CD was subdivided into two regions, and the solution grid points were generated to suit the use of the wall functions. Finer, unstructured meshes were generated via size functions for the interior subdomain, which contained the solar panel module(s). In this region, the first grid point from the solid wall is located at 0.001m with a growth factor of 1.2. In the outer region, coarser meshes were used. Successive adaptation techniques provided by (Fluent Inc., 2006) were employed to refine the mesh and bring the non-dimensional wall unit y+ between 30 and 100 units. Figure 3b illustrates the typical size of the computational domain, boundary conditions, and mesh arrangements for Case A of this study. Turbulent flows are inherently unsteady and LES captures their major properties and provide significantly more information compared to RANS (Tamura, 2008; COST; Nozu et al., 2008). Among the various sub-grid modeling techniques, dynamic Smagornisky-Lilly models and dynamic SGS kinetic energy models, which account for the transport of the sub-grid-scale turbulent kinetic energy, were used in this study. The simulation was performed using an eight parallel processor machine. A segregated solver having a Pressure Implicit with Splitting of Operators (PSIO) algorithm was used for the discretized equations. For time discretization, a second order implicit scheme was adopted. Spatial discretization is done by using the third order Quadratic Upwind Interpolation for Convective Kinematics (QUICK) difference scheme.

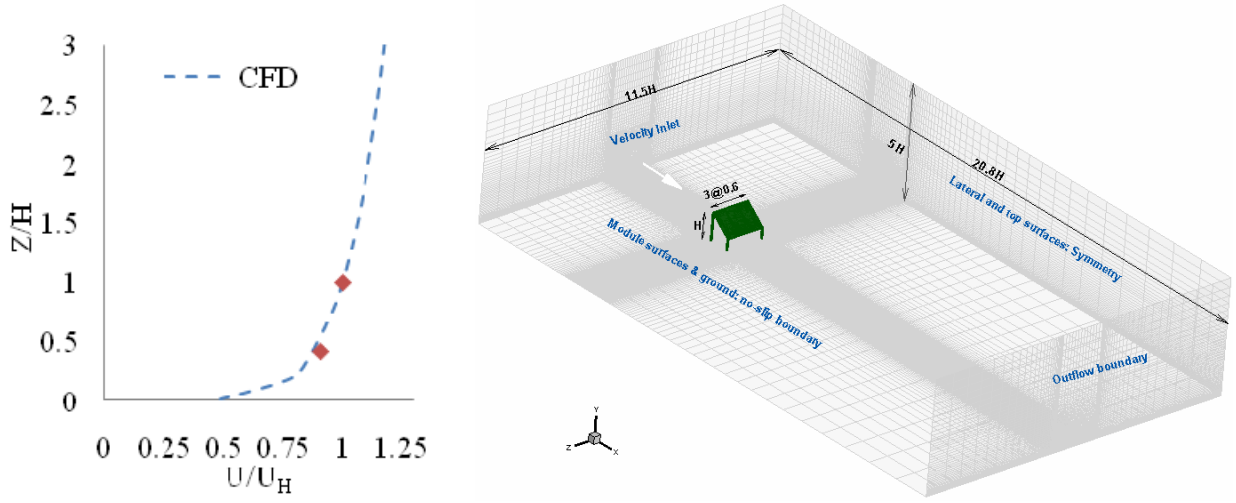

Fig 3 (a) CFD inlet velocity mean wind speed profile, and experimental wind speeds measured during the WoW experiments and (b) CD, boundary conditions and grid arrangements of stand-alone solar panel Case A

5 RESULTS AND DISCUSSION

Computationally evaluated mean pressure coefficients have been compared with full-scale measurements obtained from WoW testing at FIU. The mean pressure coefficient is defined as $C_p = 2(p-p_o)/(\rho-U_H)$, where reference pressure, p_o=1 atm was used. The reference velocity, U_H =34.5m/s, was taken at mid-height of the PV panel. Fig. 4a compares the windward face mean pressure coefficients for Case A, measured at the line indicated in Fig 4a. Although, there is some discrepancy between the CFD prediction and the full-scale measurements around the lower bottom portion of the panels, and the regions of flow separation and reattachment, the general CFD pressure coefficients follows similar pattern with the full-scale measurements. The differences between the measured results and the CFD values near the lateral beams (see Fig. 2) may be attributed to local flow modifications due to the lateral beams supporting the photovoltaic panels on the full-scale test setup, which were in close proximity to the pressure taps located near the edges of the solar panel. The CFD model did not include these horizontal beams and the CFD results were evaluated a few grid points away from the panel surfaces to minimize the effect of wall functions. Fig. 4b shows the pressure coefficients on the leeward face the solar panel for Case A. The pattern of the pressure distribution profile for the middle and exterior panels is consistent with the pattern of the full-scale measured profile. However, the magnitude of the mean pressure coefficients calculated on the exterior CFD panel show consistency with the full-scale data, unlike the pressure coefficients calculated on the middle panel. For the 0^0 wind angle of attack (Case B), the CFD predictions underestimate the wind loads at the lower portion of the solar panel, for both the windward and leeward faces (Figs 5a and b). Figures 6a and b show the mean pressure coefficients for the windward and leeward faces of the solar panel array tested in Case D. The results show significant sheltering effect by the upwind of solar panel (SP1) on the middle solar panel (SP2) and by SP1 and SP2 on the downstream solar panel (SP3). SP2 and SP3 experience negative pressure even on the windward faces. Figures 7a and b show the mean pressure contours on the solar panel surfaces for test cases A, and C, respectively. The wind pressure distributions agree with the mean pressure coefficients computed at centerline of the middle and exterior panels used for Case D SP1. For Case C, where the wind angle of attack is 30°, the corner of the panel facing the wind exhibits pressure coefficients of greater magnitude than other parts of the solar panel.

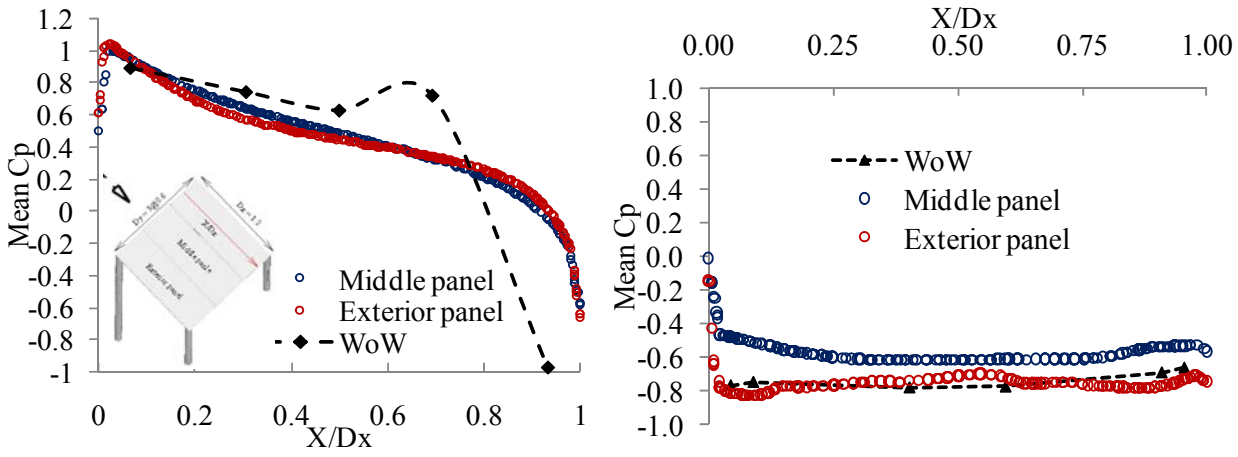

Fig 4 Comparison between CFD and WoW mean Cp on (a) windward and (b) leeward face: Case A

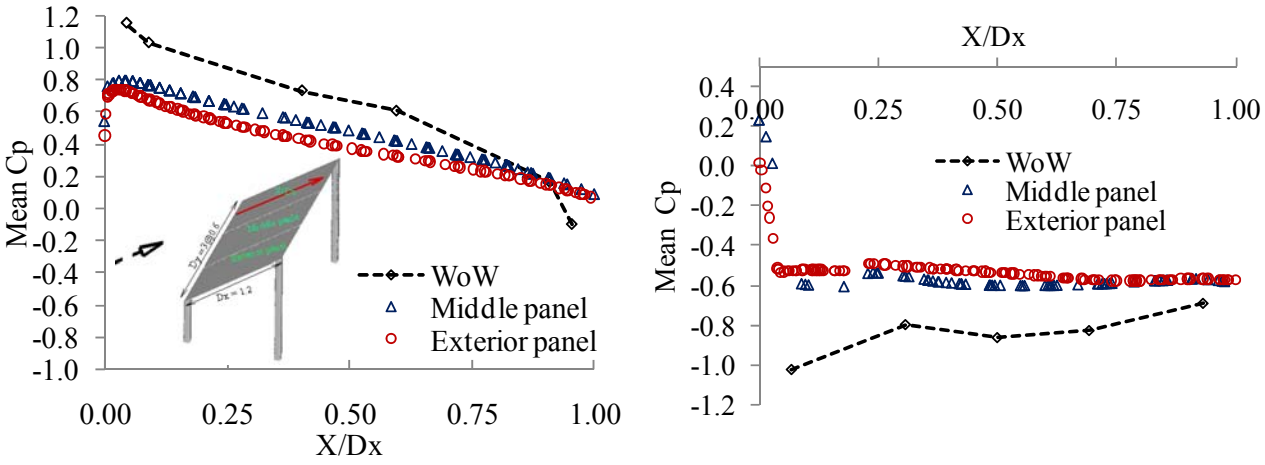

Fig 5 Comparison between CFD and WoW mean Cp on (a) windward and (b) leeward face: Case B

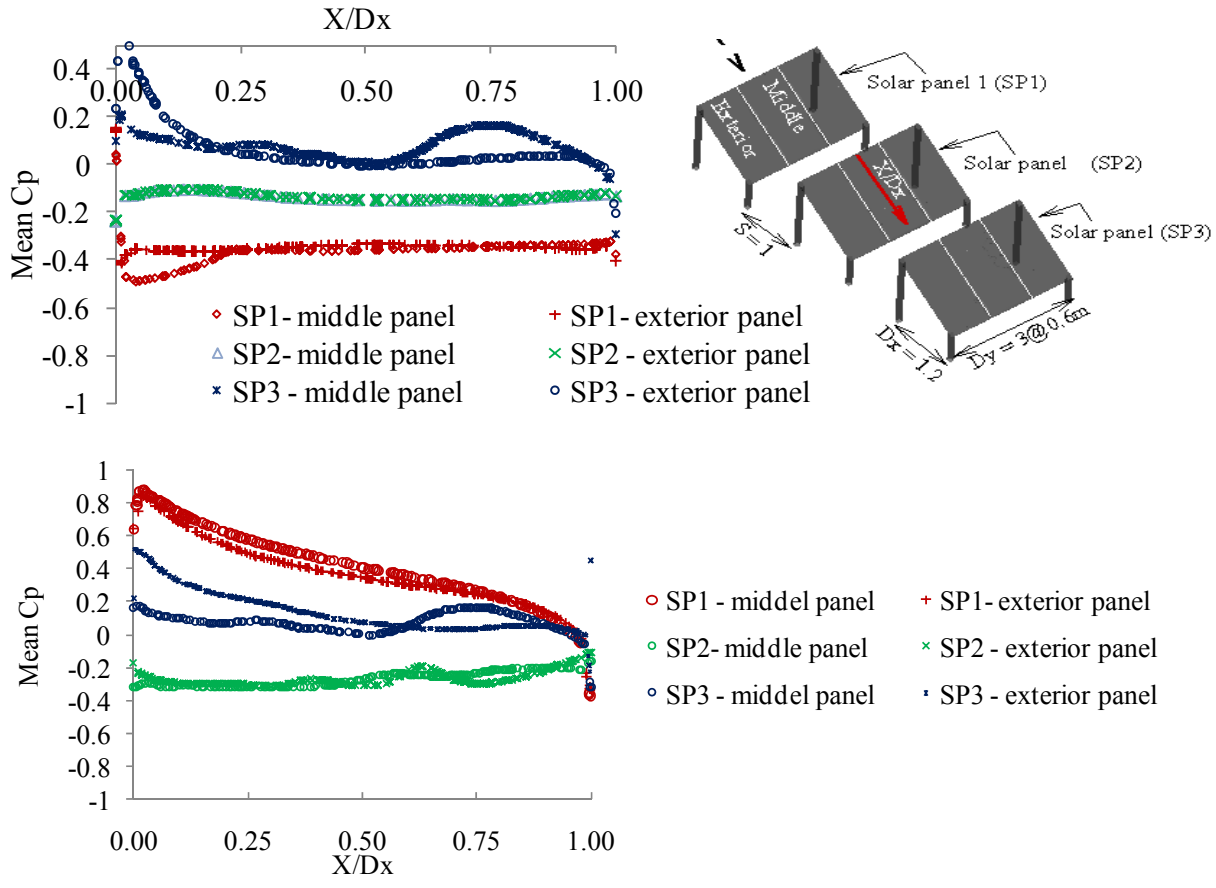

Fig 6 Comparison between WoW and CFD mean Cp on (a) leeward and (b) windward faces: Case D

To help visualize the flow, velocity contours have been plotted for representative cases. It may be observed that the fluctuating components of the flow field were captured by LES turbulence modeling and are depicted in Figure 8. Large vortices were observed in the wake region of the flow. For Case C, asymmetric flow was observed because of the oblique wind direction.

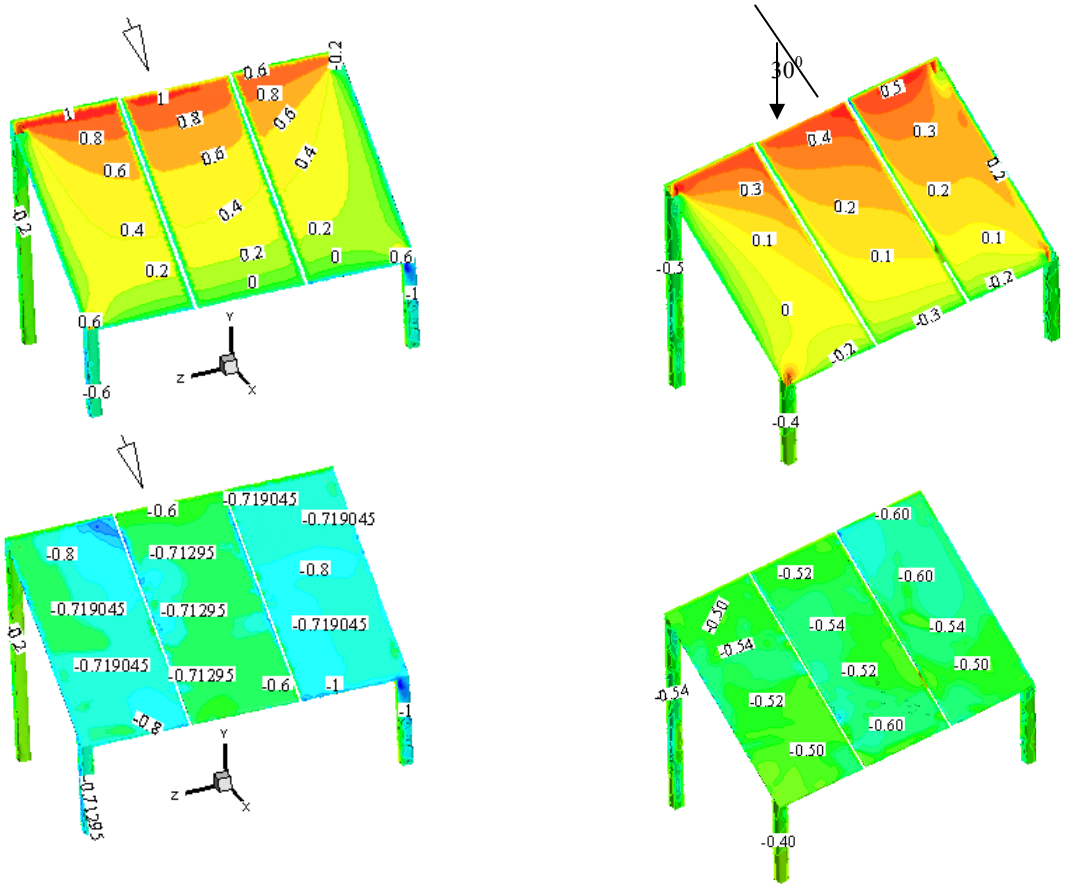

Fig 7 Mean Cp contours: Case A (left column) and Case C (right column).

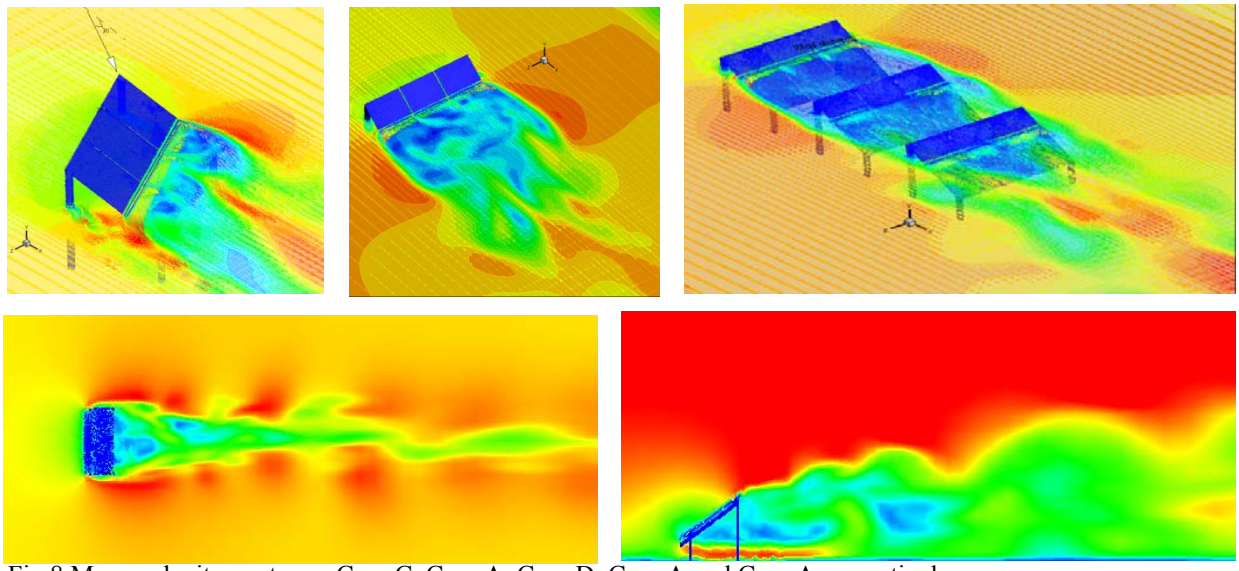

Fig 8 Mean velocity contours: Case C, Case A, Case D, Case A and Case A respectively.

6 CONCLUSION

Four different test cases have been investigated to determine the wind effects on stand-alone ground mounted solar panels differing from one another by wind angle of attack (Cases A to B) and number of panels (Case D). The numerical results obtained from CFD simulations showed similar patterns of pressure coefficient distribution when compared to full-scale measurements, but the magnitude of the pressure coefficients was generally underestimated by the numerical calculations when compared to the experimental results. The solar panels experienced the highest overall wind loads for 180^0 wind angle of attack. The study also demonstrated that a prominent sheltering effect caused by upwind solar panels substantially reduced the wind loads on the adjacent solar panel when they are arranged in tandem. For a further study, use of higher resolution mesh is necessary and may give better numerical simulation prediction accuracy.

7 ACKNOWELGMENT

Support through IHRC's Florida Center of Excellence grant is greatly acknowledged.

8 REFERENCES

Camarri, S., Salvetti, M.V., Buresti, G. 2006. Large-eddy simulation of the flow around a triangular prism with moderate aspect ratio. Journal of Wind Engineering and Industrial Aerodynamics 94, 309-322.

Chevalien, L., Norton, J. 1979. Wind loads on solar collector panels and support structure. Aerospace Engineeinrg Department, Texas A&M University.

Chung, K., Chang, K., Liu, Y. 2008. Reduction of wind uplift of a solar collector model. Journal of Wind Engineering and Industrial Aerodynamics 96, 1294-1306.

Dagnew, A.K., Bitsuamalk, G.T., Ryan, M. 2009. Computational evaluation of wind pressures on tall buildings. The 11th American conference on Wind Engineering. San Juan, Puerto Rico.

El-Okda, Y.M., Ragab, S.A., Hajj, M.R. 2008. Large-eddy simulation of flow over a surface-mounted prism using a high-order finite-difference scheme. Journal of Wind Engineering and Industrial Aerodynamics 96, 900-912.

Fluent Inc. 2006. Fluent 6.3 User's Guide. Fluent Inc., Lebanon. 6.3.26.

Huang, P., Gan Chowdhury, A., Bitsuamlak, G., Liu, R. 2009. Development of devices and methods for simulation of hurricane winds in a full-scale testing facility. Wind and Structures, Vol. 12 No 2, 151-177.

Kopp. G.A, Surry. D, Chen. K. 2002. Wind loads on solar array. Wind and Structures Vol. 5, 393-406.

Murakami, S., Mochida, A. 1988. 3-D numerical simulation of airflow around a cubic model by means of the k-ϵ model. Journal of Wind Engineering and Industrial Aerodynamics 31, 283-303.

Nozu, T., Tamura, T., Okuda, Y., Sanada, S. 2008. LES of the flow and building wall pressures in the center of Tokyo. Journal of Wind Engineering and Industrial Aerodynamics 96, 1762-1773.

Shademan, M., Hangan, H. 2009. Wind Loading on Solar Panels at Different inclination Angles. The 11th American conference on Wind Engineering. San Juan, Puerto Rico.

Stathopoulos, T. 1997. Computational wind engineering: Past achievements and future challenges. Journal of Wind Engineering and Industrial Aerodynamics 67-68, 509-532.

Tamura, T., Nozawa, K., Kondo, K. 2008. AIJ guide for numerical prediction of wind loads on buildings. Journal of Wind Engineering and Industrial Aerodynamics 96, 1974-1984.

Tominaga, Y., Mochida, A., Murakami, S., Sawaki, S. 2008. Comparison of various revised k–ε models and LES applied to flow around a high-rise building model with 1:1:2 shape placed within the surface boundary layer. Journal of Wind Engineering and Industrial Aerodynamics 96, 389-411.

Tutar, M., Celik, I. 2007. Large eddy simulation of a square cylinder flow: Modelling of inflow turbulence. Wind and Structures, Vol. 10 No. 6, 511-532.